



**HAL**  
open science

# Definition, estimation and decoupling of the overall uncertainty of the outdoor air temperature measurement surrounding a building envelope

Catalina Giraldo-Soto, Aitor Erkoreka, Laurent Mora, Amaia Uriarte, Pablo Eguía-Oller, Christopher Gorse

## ► To cite this version:

Catalina Giraldo-Soto, Aitor Erkoreka, Laurent Mora, Amaia Uriarte, Pablo Eguía-Oller, et al.. Definition, estimation and decoupling of the overall uncertainty of the outdoor air temperature measurement surrounding a building envelope. *Journal of Building Physics*, 2024, 10.1177/17442591241269195 . hal-04719876

**HAL Id: hal-04719876**

**<https://hal.science/hal-04719876v1>**

Submitted on 3 Oct 2024

**HAL** is a multi-disciplinary open access archive for the deposit and dissemination of scientific research documents, whether they are published or not. The documents may come from teaching and research institutions in France or abroad, or from public or private research centers.

L'archive ouverte pluridisciplinaire **HAL**, est destinée au dépôt et à la diffusion de documents scientifiques de niveau recherche, publiés ou non, émanant des établissements d'enseignement et de recherche français ou étrangers, des laboratoires publics ou privés.



Distributed under a Creative Commons Attribution - NonCommercial 4.0 International License

# Definition, estimation and decoupling of the overall uncertainty of the outdoor air temperature measurement surrounding a building envelope

*Journal of Building Physics*

1–35

© The Author(s) 2024



Article reuse guidelines:

[sagepub.com/journals-permissions](https://sagepub.com/journals-permissions)

DOI: 10.1177/17442591241269195

[journals.sagepub.com/home/jen](https://journals.sagepub.com/home/jen)

Catalina Giraldo-Soto<sup>1</sup> , Aitor Erkoreka<sup>1</sup> ,  
Laurent Mora<sup>2</sup>, Amaia Uriarte<sup>3</sup>,  
Pablo Eguía-Oller<sup>4</sup> and Christopher Gorse<sup>5</sup>

## Abstract

Outdoor air temperature represents a fundamental physical variable that needs to be considered when characterising the energy behaviour of buildings and its subsystems. Research, for both simulation and monitoring, usually assumes that the outdoor air temperature is homogeneous around the building envelope, and when measured, it is common to have a unique measurement representing this hypothetical homogeneous outdoor air temperature. Furthermore, the uncertainty associated with this measurement (when given by the research study) is normally limited to the accuracy of the sensor given by the manufacturer. This research aims to define and quantify the overall uncertainty of this hypothetical homogeneous outdoor air temperature measurement.

<sup>1</sup>ENEDI research group, Energy Engineering Department, Faculty of Engineering of Bilbao, University of Basque Country UPV/EHU, Bilbao, Pl. Ingeniero Torres Quevedo 1, Spain

<sup>2</sup>I2M – Institute of Mechanics and Engineering, University of Bordeaux CNRS (UMR 5295), Site ENSAM, Esplanade des Arts et Métiers, Talence, France

<sup>3</sup>TECNALIA, Basque Research and Technology Alliance (BRTA), Edificio 700 Parque Tecnológico de Bizkaia, Derio, Spain

<sup>4</sup>Department of Mechanical Engineering, Heat Engines and Fluids Mechanics, Industrial Engineering School, University of Vigo (Universidade de Vigo), Vigo, Spain

<sup>5</sup>School of Architecture Building & Civil Engineering, Loughborough University, Leicestershire, UK

## Corresponding author:

Catalina Giraldo-Soto, ENEDI research group, Energy Engineering Department, Faculty of Engineering of Bilbao, University of Basque Country UPV/EHU, Bilbao, Spain. Pl. Ingeniero Torres Quevedo 1, 48013, Bilbao, Spain.

Email: [catalina.giraldo@ehu.eus](mailto:catalina.giraldo@ehu.eus)

It is well known that there is considerable variability in outdoor air temperature around the building and measurements are dependent on the physical location of outdoor air temperature sensors. In this research work, this existing spatial variability has been defined as a random error of the hypothetical homogeneous outdoor air temperature measurement, which in turn has been defined as the average temperature of several sensors located randomly around the building envelope. Then, some of these random error sources which induce spatial variability would be the cardinal orientation of the sensor, the incidence of solar radiation, the outdoor air temperature stratification, the speed and variations of the wind and the shadows of neighbouring elements, among others. In addition, the uncertainty associated with the systematic errors of this hypothetical homogeneous outdoor air temperature measurement has been defined as the Temperature Sensor Uncertainty ( $U_{T(S)}$ ), where this uncertainty is associated with the sensor's accuracy. Based on these hypotheses, a detailed statistical procedure has been developed to estimate the overall Temperature Uncertainty ( $U_T$ ) of this hypothetical homogeneous outdoor air temperature measurement and the Temperature Sensor Uncertainty ( $U_{T(S)}$ ). Finally, an uncertainty decoupling method has also been developed that permits the uncertainty associated with random errors (Temperature's Spatial Uncertainty ( $U_{T(SP)}$ )) to be estimated, based on  $U_T$  and  $U_{T(S)}$  values. The method has been implemented for measuring the outdoor air temperature surrounding an in-use tertiary building envelope, for which an exterior monitoring system has been designed and randomly installed. The results show that the overall Temperature Uncertainty ( $U_T$ ) for the whole monitored period is equal to  $\pm 2.22^\circ\text{C}$ . The most notable result is that the uncertainty associated with random errors of measurement (Temperature's Spatial Uncertainty ( $U_{T(SP)}$ )) represents more than 99% of the overall uncertainty; while the Temperature Sensor Uncertainty ( $U_{T(S)}$ ), which is the one commonly used as the overall uncertainty for the outdoor air temperature measurements, represents less than 1%.

## Keywords

Outdoor air temperature, uncertainty, measurement, monitoring system

## Introduction

Outdoor air temperature is an intensive physical variable used for many purposes, including the energy performance of building analysis, the optimisation of Building Automation Systems (BAS) and buildings' Heating, Ventilating and Air Conditioning (HVAC) systems control. From the point of view of the building energy balance, outdoor air temperature affects the heat transfer rate occurring through the building envelope via transmission losses and infiltration/ventilation losses (Bauwens and Roels, 2014; Chapman, 1984). The building envelope Heat Transfer Coefficient (HTC) is the parameter that best represents the overall energy performance of a building envelope. The HTC is the total heat transfer from a building resulting from transmission heat transfer through the envelope and from

infiltration and/or ventilation per °C of indoor to outdoor temperature difference in W/°C. Since the HTC considers ventilation/infiltration effects, much of the variability in this estimate is due to time variability in weather conditions (Juricic et al., 2021); mainly outdoor air temperature and wind velocity. Thus, there is a need to achieve a representative measure of the temperature of the air surrounding the building envelope. This representative outdoor air temperature measure should consider the spatial variability of this measure around the building envelope and it should focus on how solar irradiation influences this spatial variability.

### *State of the art*

As detailed in Giraldo-Soto et al. (2018), the outdoor air temperature measurements are commonly collected from the closest weather station to the analysed building, or by dedicated sensors (usually only one sensor per building) installed around the building envelope (on the façade, the roof or close to the studied building). Then, these unique outdoor air temperature measurements are used to represent the outdoor air temperature as homogeneous around the building envelope for each instant of time (Giraldo-Soto et al., 2018). Thus, it is considered or assumed that the air temperature surrounding a building only varies with time. Furthermore, the overall uncertainty associated with these outdoor air temperature measurements is considered to be the manufacturer's accuracy of the sensors.

For example, in Yang et al. (2020), an experimental test was conducted on the campus of Nanyang Technological University in Singapore to study a model predictive control approach for an air conditioning system with a dedicated outdoor air system. To be able to model the air conditioning system demands, a dynamic model of the tested building area was constructed; where one of the main inputs for the model was the locally measured outdoor air temperature. To carry out the test, the outdoor air temperature of the building was measured, with the uncertainty due to systematic errors equal to  $1/3\text{DIN}$ , this value being the manufacturer's accuracy, without taking into account other uncertainty sources. In the case of Housez et al. (2014), large discrepancies were found between the real and the design heating demands of seven energetically retrofitted buildings located in Austria. The analysis compared the buildings' real heating demands (estimated based on energy bills) against the heating demands obtained by different energy certificate methodologies and by simulating the heating demand of the analysed buildings. In the simulation, among others, the outdoor air temperature was one of the main input variables. In this study, the outdoor air temperature data was collected from weather stations close to the analysed buildings, without specifying their exact location regarding the analysed buildings or the manufacturer's accuracy of the sensor. Similarly, in Chung et al. (2023), the variation in the building envelope moisture behaviour was studied using simulation work with multi-year historical weather data. This study demonstrated that envelope hygrothermal simulations using single-year moisture reference years, and single-trial climate, might underestimate moisture content and moisture-related damage as compared to simulations using stochastic simulations.

In this study case, there are neither technical specifications of the weather station nor the manufacturer's accuracy or sensor location concerning the demo test.

Another example is Vivek and Balaji (2023), which studied the cooling behaviour of a Thermally Activated Building System (TABS). For this purpose, they experimentally evaluated the effect on the indoor air temperature, surface temperature and heat transfer rate in a room with TABS and compared the results with an uncooled identical room. The outdoor air temperature variations were identified to define the cooling scenarios. In this research work, the manufacturer's accuracies and the Type B uncertainties of surface temperature sensors, heat index meters, heat flux sensors and digital anemometers are shown, together with the estimation of the uncertainties of the radiant temperature and the operating temperature. However, the study does not include the manufacturer's accuracy or the uncertainty of the weather parameters (outdoor air temperature, relative humidity and solar radiation) collected from a weather station located in front of the experimental facility. Likewise, in Jack et al. (2018), seven teams independently conducted co-heating tests on the same detached house near Watford, UK, to estimate its Heat Transfer Coefficient (HTC). This study empirically demonstrates the reliability of the co-heating test. The uncertainty of the estimated building envelope heat transfer coefficients was obtained with different methods. In these tests, for the outdoor air temperature measurement, only the uncertainty associated with a systematic error equal to  $\pm 0.2^\circ\text{C}$  (the manufacturer's sensor accuracy) is given. However, an uncertainty equal to  $\pm 1^\circ\text{C}$  was assumed in the indoor-to-outdoor air temperature difference measurement, without specifying the way this uncertainty was obtained.

Another case is Ghosh et al. (2015), where the overall heat transfer coefficient (*U*-value) of two glazing systems under the same conditions was estimated. For this, two identical test cells were designed, manufactured and installed at the Dublin Energy Laboratory. For the test, the indoor and outdoor conditions were monitored, where a T-type thermocouple was installed to measure the outdoor air temperature, without specifying its location. Once again, only the manufacturer's accuracy of the outdoor air temperature sensor is considered, it being equal to  $\pm 1^\circ\text{C}$ . In another case, Sougkakis et al. (2021), the HTC was estimated by testing the Quick U-Building method for assessing the HTC in two UK buildings. The outdoor air temperature as a variable was included for estimating the HTC, measured via a weather station installed on the roof of a neighbouring house, approximately 30 m from the test house. The manufacturer's accuracy of outdoor air temperature is not shown, but only the uncertainty of the heat transfer coefficients are specified through the standard deviations of their mean values. Similarly, Lai et al. (2020) presents a three-dimensional integrated numerical model to evaluate the building's surface and mean radiant temperature. For this study, only one outdoor air temperature sensor with a manufacturer's accuracy of  $\pm 0.20^\circ\text{C}$  was installed on the roof of a building; this sensor was not shielded against radiation and was located in a shaded area to avoid the incidence of direct solar radiation. In Li et al. (2023), to size an air source heat pump, two models (under non-frosting and frosting conditions), considering the joint effect of outdoor air temperature and relative humidity,

were developed to predict the output heating capacity of the analysed heat pump units. Experimental tests were conducted in a small office building in Beijing to validate the accuracy of the said models. The measurement system was built up to monitor and record the operating parameters of the tested air source heat pump units, where the outdoor air temperature sensor used was the model QFM9160. Once again, only the uncertainty due to systematic error was taken into account, this being equal to  $\pm 0.15^{\circ}\text{C}$ .

In a case study of Chinese residential buildings (Yan et al., 2016), the influence of the outdoor air temperature on the indoor environment and thermal adaptation was studied. Through the thermal comfort questionnaire, the dwelling occupants defined the subjective thermal sensation with the ASHRAE seven-point scale, and then a statistical analysis was undertaken to analyse the influence of outdoor air temperature on thermal comfort. The study does not specify the layout of the single outdoor air temperature sensor and only mentions the manufacturer's accuracy of the outdoor air temperature sensor being equal to  $\pm 0.5^{\circ}\text{C}$ . In Calama-González et al. (2021), the influence of ventilation on indoor comfort was evaluated. In this study, several ventilation protocols (natural and mechanical) were analysed to determine how they can affect the indoor environmental variables. These indoor environments were monitored in two independent test cells with a window located in the South face, where the ventilation occurs. To define ventilation protocols, the correlation between the indoor and outdoor air temperature gradients was one of the assessed parameters. Therefore, the outdoor air temperature measurement, with a manufacturer's precision equal to  $\pm 0.15^{\circ}\text{C}$ , was measured from a single weather station located on the roof of one of the two independent cells. Only the manufacturer's accuracy is mentioned in this study.

In research (Bakkush et al., 2015), where the effect of the outdoor air temperature on the thermal performance of a residential building was studied, sensors were located outside the building to compare the geographical outdoor air temperature surrounding the façades and roof with the outdoor average temperature based on the collected data. This study does not specify the sensor model or the manufacturer's accuracy, and even where there are several outdoor air temperature measurements, there is no definition or quantification of an overall outdoor air temperature measurement uncertainty. Similarly, sensor accuracy and uncertainty are overlooked in research (Sansaniwal et al., 2021) which focused on the adaptive actions of occupants to control the indoor environment in naturally ventilated buildings. This study used the correlation between indoor and outdoor air temperatures to analyse the window opening behaviour related to environmental conditions. The study was conducted in naturally ventilated office buildings and hostels located within a radius of 10 km in the city of Jaipur, without specifying the number or location of the buildings studied, or the sensor used to measure the outdoor air temperature. There is also no mention of the manufacturer's sensor accuracy. The same applies in Borkowski and Piłat (2022), where the design of a refrigeration system and its control was studied, with a comprehensive analysis of compressor and free cooling modes to demonstrate the adaptation of the existing demand to

outdoor temperatures in the climate of the Małopolska Province, which has significant temperature fluctuations. In this experimental test, an outdoor temperature sensor was located on the roof of the building in a shaded place, but neither the type of sensor or its manufacturer's accuracy is specified.

Furthermore, in other non-building case studies, little consideration is given to external temperature measurements; such as the research (He et al., 2020) undertaken on the outdoor air temperature entering a tunnel with a  $78.5\text{ m}^2$  cross-sectional area represented by just one air temperature sensor located 100 m away from the tunnel entrance and with a manufacturer's accuracy of  $\pm 0.50^\circ\text{C}$ . Similarly, other studies (Huang et al., 2020) addressing the impact of different ground surfaces on thermal environments in outdoor activity spaces did not fully consider the variability and uncertainty of the external environment temperature. Five different measurement areas with different ground surfaces were measured and studied simultaneously. The outdoor air temperature was measured with a single weather station for each ground surface at the height of 1.1 m, with a manufacturer's accuracy equal to  $\pm 0.30^\circ\text{C}$ . Similar oversights are observed in research (Zhang et al., 2020) that studied the correlation between air temperature and urban morphology parameters in a cold climate city in China. The outdoor microclimate was evaluated through 27 measurement points located in open areas, using air temperature sensors with a manufacturer's precision equal to  $\pm 0.20^\circ\text{C}$ . In this study, only the horizontal stratification of the outdoor air temperature was considered, without the incidence of vertical stratification, as the experimental set-up placed the sensors in a grid with a distance of 100–200 m and at the height of less than 1.5 m. Furthermore, the work does not relate the measurements' spatial variability with an uncertainty estimation of the hypothetical homogeneous outdoor air temperature representative for the whole analysed area.

In the same way, the International Organization for Standardization (ISO) and the American Society of Heating, Refrigerating & Air-Conditioning Engineers (ASHRAE) state, in their standards and manuals, the importance of considering measurement uncertainties and errors, where both outdoor and indoor air temperatures are essential physical variables used to develop procedures, methodologies and calculations for buildings and their subsystems. For example, the ASHRAE Handbook Fundamentals (ASHRAE, ) speaks about the importance of uncertainty estimation and highlights that 'knowing the type of uncertainty associated with a parameter is important in understanding how to propagate that uncertainty through the model'. Its Chapter 28: 'Heat, air, and moisture control in buildings', specifies that 'the annual calibration certificate is essential', where the measurement uncertainty should be included, but does not specify how to estimate it or what the incidence of systematic and random errors is on this. However, these errors are defined in Chapter 38: 'Measurement and instruments'. In turn, Chapter 38 also shows the uncertainty of temperature measurements in Table 1, 'Common Temperature Measurement Techniques', which only specifies the uncertainties associated with systematic errors (the manufacturer's sensor accuracy). In the same way as the ASHRAE Handbooks, the normative of ISO 9869-1 (ISO Standard

**Table 1.** Technical characteristics of the sensors, gateway and protocol communications of the MMS.

Sensor reference	Measure	Accuracy	Protocol communication
EE + Plus EE071-HTPC <sup>1</sup> (E + E Elektronik Ges.m.b.H., )	Temperature	$\pm 0.1^{\circ}\text{C}$ at $23^{\circ}\text{C}$	Digital – Modbus RS485
	Relative Humidity	$\pm 2\%$ RH (0...90% RH) $\pm 3\%$ RH (0...100% RH)	
<b>Gateway</b>			
Reference	Producer	Protocols	Description
KNXRTUIK (DEEI, )	DEEI	KNX to Modbus RTU-RS485	RS485 Half-Duplex interface for Modbus RTU. The 120-ohm RS485 termination resistor inside the gateway. Operating temperature $-40^{\circ}\text{C}$ to $+85^{\circ}\text{C}$ . Maximum number of points 1000. Supports Boolean data, 8 bits, 16 bits, 32 bits, 64 bits, float 16, float 32

Source: Based on Giraldo-Soto et al. (2020).

<sup>1</sup>The manufacturer's reference corresponding to the old EE071-HTPC reference is currently EE072-HS1TT1F32J3 (E + E Elektronik Ges.m.b.H., ).

9869-1, 2014) specifies that the accuracy of the estimated transmittance values depends on the environment temperature measurements (indoor and outdoor air temperature), but does not explain a methodology to estimate outdoor air temperature measurement uncertainty due to systematic and random errors.

### *Aim and research questions*

All of the above from normative and research works demonstrates that representing the outdoor air temperature surrounding a building envelope, the air temperature of a tunnel section or even the temperature of an urban zone as homogeneous is widespread. In such studies, the outdoor air temperatures are commonly measured with a single sensor, and when given, the uncertainty associated with these measurements is simply the manufacturer's accuracy.

This research aims to quantify the correctness of this approach for the specific case of the outdoor air temperature surrounding a building envelope (note that the method would also be valid for the other non-building cases mentioned). To do so, the hypothetical homogenous outdoor air temperature surrounding a building



envelope at a given instant of time is defined as the average temperature of several sensors located randomly around the building envelope (from now on named  $T_{out}$ ). This average temperature will be the representative value of the outdoor air temperature surrounding the building, and the overall uncertainty of this measurement (namely, Temperature Uncertainty ( $U_T$ )) is obtained from the total variability of the individual measurements regarding this average for each instant of time. This total variability will have two sources: variability due to the sensors' accuracy (these shall be considered as systematic errors) and variability due to physical effects occurring around the building envelope that generate spatial variability of the outdoor air temperature surrounding a building (these shall be considered as random errors).

Furthermore, the method also details the way in which the uncertainty associated with systematic errors can be estimated based on the manufacturer's accuracy, and this is called the Temperature Sensor Uncertainty ( $U_{T(S)}$ ). Moreover, based on ( $U_T$ ) and ( $U_{T(S)}$ ) values, an uncertainty decoupling method has also been developed to estimate the uncertainty associated with random errors (namely the Temperature's Spatial Uncertainty ( $U_{T(SP)}$ )). This uncertainty study is based on the GUM method (BIPM).

Finally, the method was implemented for an in-use tertiary building, where eight high-precision outdoor air temperature sensors were randomly installed around the building envelope to take simultaneous measurements at different heights and cardinal orientations for several weeks. This uncertainty analysis of the temperature of the air surrounding the building also focuses on analysing the overall measurement uncertainty of  $T_{out}$  when considering sub-periods with high and low solar irradiation. The latter analysis is fundamental to understand important reliability aspects when selecting the periods to estimate the HTC.

## Method

This section explains the statistical method used to estimate the uncertainty of  $T_{out}$ ; for this, the state of the art of the applied method is first set out, followed by an explanation of the methodology used to estimate the different measurement uncertainties of  $T_{out}$ :

- Overall  $T_{out}$  measurement uncertainty, identified as 'Temperature Uncertainty ( $U_T$ )'.
- The uncertainty due to systematic errors in the  $T_{out}$  measurement, identified as 'Temperature Sensor Uncertainty ( $U_{T(S)}$ )'.
- The measurement uncertainty due to random fluctuations occurring in the building envelope is identified as 'Temperature's Spatial Uncertainty ( $U_{T(SP)}$ )'. This uncertainty is estimated by decoupling the estimated overall Temperature Uncertainty ( $U_T$ ) with the Temperature Sensor Uncertainty ( $U_{T(S)}$ ).

In this study, to estimate the temperature uncertainty in open exterior volumes, the same method used for closed interior volumes (Giraldo-Soto et al., 2022) has been implemented. Even if the estimation of the overall uncertainty is similar; in this work, it has been proven that decoupling this overall uncertainty is also possible without doing the Sensor Together Test to obtain the systematic uncertainty. In this case, the systematic uncertainty has been estimated starting from the manufacturer's accuracy value.

### *State of the art of uncertainty analysis methods*

The statistical method to estimate the measurement uncertainty of  $T_{\text{out}}$  is based on the GUM method for a distribution Type A (BIPM, ), which is made up of a sample with independent observation series of 30 or more. The Standard Uncertainty ( $U$ ) in the statistical analysis of the Type A assessment is the measurement uncertainty expressed in terms of a sample's Mean Standard Deviation ( $U = \bar{\sigma}$ ), where it is possible to obtain an 'Expanded Uncertainty' if this  $U$  value is multiplied by a Coverage Factor ( $k$ ), which is expected to be within the 95% confidence level interval if the  $k$ -value is equal to 2 ( $\bar{U} = 2\bar{\sigma}$ ), or 99% if it is equal to 3 ( $\bar{U} = 3\bar{\sigma}$ ) (BIPM, ).

All uncertainties set out in this study ( $U_T$ ,  $U_{T(S)}$  and  $U_{T(SP)}$ ) have been estimated within the 95% confidence level interval using the  $k$ -value equal to 2 ( $\bar{U} = 2\bar{\sigma}$ ).

### *Temperature Uncertainty ( $U_T$ ) analysis*

The outdoor air temperature measurements carried out around an in-use tertiary building are analysed in this manuscript (these data sets are available in the 'Exterior (E) Test' files of reference (Giraldo-Soto et al., 2020)). The statistical study samples are the Instants of Time ( $t_j$ ). In each ( $t_j$ ),  $Z$  measurements of outdoor air temperature have been acquired from sensors installed on four Building Areas (BA) of the envelope: the roof and three façades facing north, south and west. These temperature values are the Sensor Temperature Measurements ( $T_{dv_i}$ ), which are defined as a temperature value into a Differential Volume ( $dv_i$ ) of a monitored zone, in which, in turn, the  $dv_i$  represents the volume where a temperature sensor is located.  $T_{dv_i}$  represents one measurement point of the whole air volume surrounding the building envelope, called in this manuscript Building Air Volume (BAV), where the Total Average Temperature of the whole BAV ( $(T_a)_{ta}$ ) is defined by the sum of  $p$  units of  $T_{dv_i}$  measurement in the whole BAV divided by  $p$  (equation (1)). In addition, the Local Average Temperature of a BA ( $(T_a)_{la}$ ) is defined by the sum of  $q$  units of  $T_{dv_i}$  measurement in a BA divided by  $q$  (equation (2))

The uncertainty analysis method applied in this study is based on the following steps (Figure 1; Giraldo-Soto, 2021):

- (1) The statistical analysis to estimate the uncertainty of  $T_{\text{out}}$  must be performed at  $T_{dv_i}$  values centred on an Average Temperature ( $T_a$ ) (in this work with respect to BAV  $(T_a)_{ta}$  or BA  $(T_a)_{la}$ ); for which equation (3) or (4) is

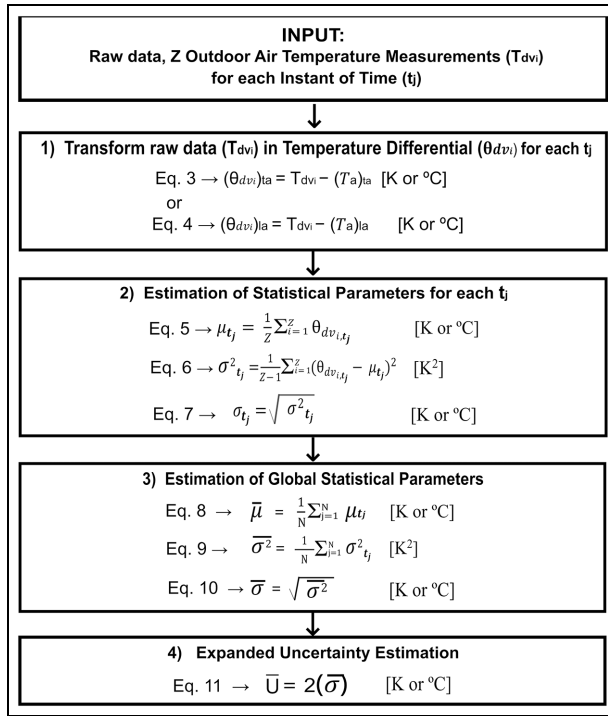


**Figure 1.** Flowchart of the methodology to estimate the Temperature Uncertainty ( $U_T$ ) of  $T_{out}$ . Based on (Giraldo-Soto et al., 2022).

used, respectively, in order to have a new temperature value in each measurement point, which is called the Temperature Differential ( $\theta_{dvi}$ ),  $((\theta_{dvi})_{ia})$  for data centred on  $(T_a)_{ia}$  or  $(\theta_{dvi})_{ia}$  if the data is centred on  $(T_a)_{ia}$ . From this point on, each Instant of Time ( $t_j$ ) has  $Z$  new temperature values (the Temperature Differentials ( $\theta_{dvi}$ )) and it is therefore possible to consider the hypothesis that instants of time ( $t_j$ ) are independent of each other, since only the centred temperature differentials are considered within each Instant of Time. The study's large sample size ensures that the data collected follows a type A distribution. Two dimensions are combined in the sample; the spatial dimension, by locating several sensors randomly around the building envelope, and the time, by taking measurements for an extended period with a specific frequency. This combination permits a large sample to be obtained that tends towards a normal distribution.

- (2) Estimation of the mean ( $\mu$ ) (equation (5)), standard deviation ( $\sigma$ ) (equation (6)) and variance ( $\sigma^2$ ) (equation (7)) values, for  $N$  Instants of Time ( $t_j$ ) with  $Z$  units of  $\theta_{dvi}$  values in each of those instants of time.

- (3) The Global Mean ( $\bar{\mu}$ ) (equation (8)), Mean Variance ( $\overline{\sigma^2}$ ) (equation (9)) and the Mean Standard Deviation ( $\bar{\sigma}$ ) (equation (10)) are estimated.
- (4) Based on the GUM method (BIPM, ), the Temperature Uncertainty ( $U_T$ ), with a confidence interval of 95%, is obtained by multiplying  $\bar{\sigma}$  by  $k = 2$  (equation (11)).
- (5) The statistical parameters of this study have been calculated to obtain the results of Section ‘Results and discussions’, using Scispy-stats (Scipy,), Pandas libraries (Pandas,) and programming in Python (Python.org.).

$$(T_a)_{ta} = \sum_{i=1}^p \frac{T_{dv_i}}{p} \text{ [K or } ^\circ\text{C]} \quad (1)$$

$$(T_a)_{la} = \sum_{i=1}^q \frac{T_{dv_i}}{q} \text{ [K or } ^\circ\text{C]} \quad (2)$$

$$(\theta_{dv_i})_{ta} = T_{dv_i} - (T_a)_{ta} \text{ [K or } ^\circ\text{C]} \quad (3)$$

$$(\theta_{dv_i})_{la} = T_{dv_i} - (T_a)_{la} \text{ [K or } ^\circ\text{C]} \quad (4)$$

Where,

$T_{dv_i}$ :  $i$ th Sensor Temperature Measurement for each  $t_j$  [K or  $^\circ\text{C}$ ].

$T_a$ : Average Temperature of a BAV or a BA for each  $t_j$  [K or  $^\circ\text{C}$ ].

$(T_a)_{ta}$ : Total Average Temperature of the BAV for each  $t_j$  [K or  $^\circ\text{C}$ ].

$(T_a)_{la}$ : Local Average Temperature of a BA for each  $t_j$  [K or  $^\circ\text{C}$ ].

$p$ : Number of  $T_{dv_i}$  measurements in the BAV for each  $t_j$ .

$q$ : Number of  $T_{dv_i}$  measurements in a BA for each  $t_j$ .

$\theta_{dv_i}$ : Temperature Differential for each  $t_j$  [K or  $^\circ\text{C}$ ].

$(\theta_{dv_i})_{ta}$ : Temperature Differential of  $T_{dv_i}$  centred on the  $(T_a)_{ta}$  for each  $t_j$  [K or  $^\circ\text{C}$ ].

$(\theta_{dv_i})_{la}$ : Temperature Differential of  $T_{dv_i}$  centred on the  $(T_a)_{la}$  for each  $t_j$  [K or  $^\circ\text{C}$ ].

$$\mu_{t_j} = \frac{1}{Z} \sum_{i=1}^Z \theta_{dv_{i,t_j}} \text{ [K or } ^\circ\text{C]} \quad (5)$$

$$\sigma^2_{t_j} = \frac{1}{Z-1} \sum_{i=1}^Z (\theta_{dv_{i,t_j}} - \mu_{t_j})^2 \text{ [K}^2\text{]} \quad (6)$$

$$\sigma_{t_j} = \sqrt{\sigma^2_{t_j}} \text{ [K or } ^\circ\text{C]} \quad (7)$$

$$\bar{\mu} = \frac{1}{N} \sum_{j=1}^N \mu_{t_j} \text{ [K or } ^\circ\text{C]} \quad (8)$$

$$\bar{\sigma}^2 = \frac{1}{N} \sum_{j=1}^N \sigma^2_{t_j} \text{ [K}^2\text{]} \quad (9)$$

$$\bar{\sigma} = \sqrt{\bar{\sigma}^2} \text{ [K or } ^\circ\text{C]} \quad (10)$$

$$U = 2(\bar{\sigma}) \text{ [K or } ^\circ\text{C]} \quad (11)$$

Where,

$\theta_{d_{vi},t_j}$ : Temperature Differential, defined by the difference between each  $T_{d_{vi}}$  concerning  $(T_a)_{ia}$  or  $(T_a)_{la}$  for each  $t_j$  [K or °C].

$\mu_{t_j}$ : Mean of Temperature Differentials ( $\theta_{d_{vi}}$ ) for each  $t_j$  [K or °C].

$\sigma^2_{t_j}$ : Variance of Temperature Differentials ( $\theta_{d_{vi}}$ ) for each  $t_j$  [K<sup>2</sup>].

$\sigma_{t_j}$ : Standard Deviation of Temperature Differentials ( $\theta_{d_{vi}}$ ) for each  $t_j$  [K or °C].

$\bar{\mu}$ : Global Mean or Mean of  $N \mu_{t_j}$  [K or °C].

$\bar{\sigma}^2$ : Mean Variance of  $N \sigma^2_{t_j}$  [K<sup>2</sup>].

$\bar{\sigma}$ : Mean Standard Deviation of the sample, this value is associated with the Temperature Uncertainty estimation [K or °C].

Z: Number of  $T_{d_{vi}}$  measurements in a BAV ( $Z = p$ ) or a BA ( $Z = q$ ) volume for each  $t_j$ .

N: Sample Size defined by the number of Instants of Time ( $t_j$ ).

In the case where there is only one sensor temperature measurement ( $Z = 1$ ), the  $T_{d_{vi}}$  values cannot be centred with respect to a reference temperature, so the proposed statistical analysis cannot be applied.

*Temperature Uncertainty ( $U_T$ ) analysis for outdoor air temperature measurements protected with solar radiation shield with and without mechanical ventilation.* This first analysis demonstrates that the solar radiation-shielded outdoor air temperature sensors only measure the convection air temperature, excluding any solar radiation effect on these temperature measurements. Solar radiation shields without mechanical ventilation are commonly used to protect outdoor air temperature sensors against solar radiation effects on their measurements. In this research, one of the temperature sensors has been protected by a mechanically ventilated solar shield, while naturally ventilated solar radiation shields have protected the rest. Thus, it has been possible to demonstrate that the not mechanically ventilated solar radiation-protected air temperature measurements are not affected by solar radiation. For this, two sensors, one with mechanically ventilated solar shielding and the other with naturally ventilated solar shielding, were installed in the same place, measuring next to each other in a BA at the same height. Then, the Temperature Uncertainty ( $U_T$ ) for these two sensors was estimated for a sample with  $N$  Instants of Time  $t_j$ , where the  $T_{d_{vi}}$  measurements were centred on  $(T_a)_{ia}$  to obtain the new data values,  $(\theta_{d_{vi}})_{ia}$ . The statistical analysis was applied to the  $(\theta_{d_{vi}})_{ia}$  values based on the methodology explained in Subsection ‘Temperature Uncertainty ( $U_T$ ) analysis’.

*$T_{out}$  overall Temperature Uncertainty ( $U_T$ ) estimation for the whole Building Air Volume (BAV).* In order to estimate the overall temperature Uncertainty ( $U_T$ ) of  $T_{out}$  surrounding the building, or BAV, the statistical analysis was applied to the  $p$   $T_{d_{vi}}$  measurements from all the sensors installed around the building envelope. These  $T_{d_{vi}}$  data were centred on  $(T_{d_{vi}})_{ia}$ , obtaining  $(\theta_{d_{vi}})_{ia}$  values for each  $t_j$ . The statistical analysis implemented to obtain the overall Temperature Uncertainty ( $U_T$ ) is described in Subsection ‘Temperature Uncertainty ( $U_T$ ) analysis’. The obtained uncertainty value includes all systematic and random uncertainty sources affecting  $T_{out}$ . The analysis was performed for the whole data series; however, two filters

were applied to also obtain the overall temperature Uncertainty ( $U_T$ ) considering only sunny hours and only periods without solar radiation. Where the sunny periods are the  $t_j$  with measured global horizontal solar radiation values greater than  $50 \text{ W/m}^2$  and the non-sunny periods with values less than  $50 \text{ W/m}^2$ .

**Temperature Sensor Uncertainty ( $U_{T(S)}$ ) analysis.** This analysis aims to estimate the uncertainty sources due to systematic errors of the installed sensors. In this case, eight newly calibrated high-accuracy sensors from the same batch were acquired. Furthermore, the selected sensors are digital, so no uncertainty associated with the monitoring system connections is expected and thus, the Temperature Sensor Uncertainty ( $U_{T(S)}$ ) is considered as the sensor's accuracy ( $0.1^\circ\text{C}$ ), estimated experimentally by the manufacturer. The coverage factor of the manufacturer for the accuracy estimation is  $k = 2$ , so the standard deviation of the Temperature Sensor Uncertainty ( $U_{T(S)}$ ) can be estimated using equation (11) and the variance by applying equation (10).

### **Decoupling the overall Temperature Uncertainty ( $U_T$ ) by means of the Temperature Sensor Uncertainty ( $U_{T(S)}$ ) to estimate the Temperature's Spatial Uncertainty ( $U_{T(SP)}$ ) for the whole Building Air Volume (BAV)**

Temperature Uncertainty ( $U_T$ ) (equation (11)) can be decoupled, since the  $U_{T(S)}$  value is independent of the rest of the causes of temperature uncertainty,  $U_{T(SP)}$ , and both uncertainties make up the Temperature Uncertainty ( $U_T$ ) value (Giraldo-Soto, 2021). Then, as shown in equation (12), the total variance can be represented as the sum of the Mean Variance due to Temperature Sensor Uncertainty  $U_{T(S)}$  (systematic errors) plus the Mean Variance associated with the Temperature's Spatial Uncertainty ( $U_{T(SP)}$ ) (random errors; Giraldo-Soto, 2021).

The objective of applying the decoupling method is to obtain the Temperature's Spatial Uncertainty ( $U_{T(SP)}$ ) of the BAV, the following steps are carried out to apply the decoupling method (Figure 2):

- (1) From the experimental test,  $U_T$ ,  $\overline{\sigma^2_T}$  and  $\overline{\sigma_T}$  values are estimated, while the  $\overline{\sigma^2_{(S)}}$  and  $\overline{\sigma_{(S)}}$  statistical parameters are obtained from the  $U_{T(S)}$  value given by the manufacturer's accuracy. Equations (9) to (11) must be used.
- (2) The Mean Variance  $\overline{\sigma^2_{(SP)}}$  value associated with  $U_{T(SP)}$  is estimated with equation (13), then with equation (14) the  $\overline{\sigma_{(SP)}}$  value is calculated; finally multiplying it by two, the Temperature's Spatial Uncertainty ( $U_{T(SP)}$ ) is estimated through equation (11).
- (3) Subsequently, the weight of the systematic ( $U_{T(S)}$ ) and random ( $U_{T(SP)}$ ) causes concerning the overall uncertainty sources (Giraldo-Soto, 2021) can be estimated. For this, using equations (16) and (17), the Sensor Ratio ( $R_S$ ) and the Spatial Ratio ( $R_{SP}$ ), respectively, are obtained.

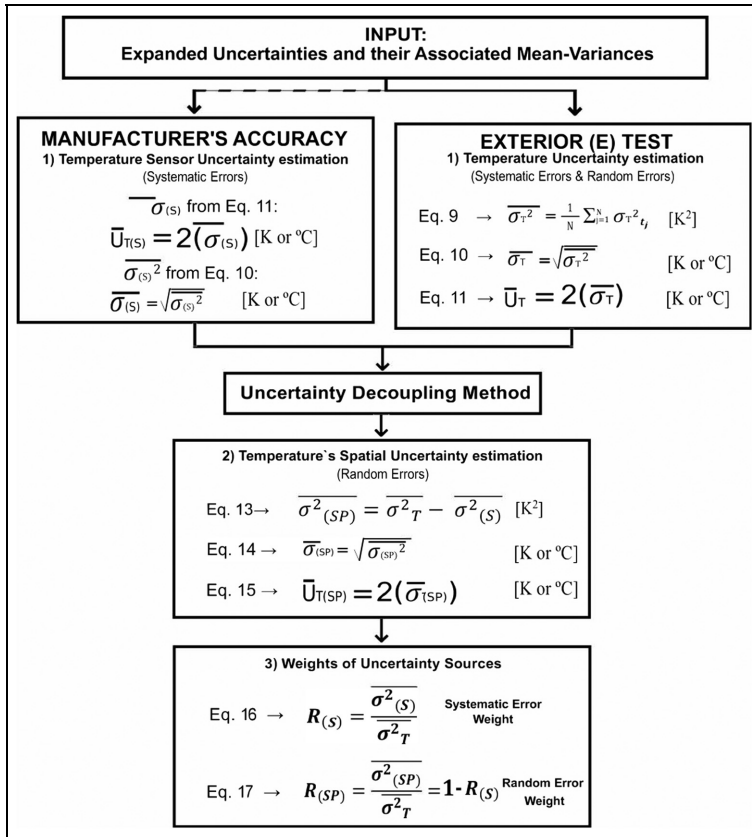


**Figure 2.** Flowchart of the decoupling methodology to estimate the Temperature's Spatial Uncertainty ( $U_{T(SP)}$ ) and the uncertainty weights. Based on Giraldo-Soto et al. (2022).

$$\overline{\sigma^2}_T = \overline{\sigma^2}_{(S)} + \overline{\sigma^2}_{(SP)} \quad [\text{K}^2] \quad (12)$$

$$\overline{\sigma^2}_{(SP)} = \overline{\sigma^2}_T - \overline{\sigma^2}_{(S)} \quad [\text{K}^2] \quad (13)$$

$$(\overline{\sigma}_{(SP)}) = \sqrt{\overline{\sigma^2}_{(SP)}} \quad (14)$$

$$\overline{U}_{T(SP)} = 2(\overline{\sigma}_{(SP)}) \quad [\text{K or } ^\circ\text{C}] \quad (15)$$

$$R_S = \frac{\overline{\sigma^2}_{(S)}}{\overline{\sigma^2}_T} \quad (16)$$

$$R_{SP} = \frac{\overline{\sigma^2}_{(SP)}}{\overline{\sigma^2}_T} = 1 - R_S \quad (17)$$

Where,

$U_T$ : Temperature Uncertainty [K or °C].

$\overline{\sigma_T^2}$ : Mean Variance of the sample associated with  $U_T$  [K<sup>2</sup>].

$\overline{\sigma_T}$ : Mean Standard Deviation of the sample, this value is associated with  $U_T$  [K or °C].

$U_{T(SP)}$ : Temperature's Spatial Uncertainty [K or °C].

$\overline{\sigma^2_{(SP)}}$ : Mean Variance of the sample associated with  $U_{T(SP)}$  [K<sup>2</sup>].

$\overline{\sigma_{(SP)}}$ : Mean Standard Deviation of the sample associated with the Temperature's Spatial Uncertainty ( $U_{T(SP)}$ ) [K or °C].

$U_{T(S)}$ : Temperature Sensor Uncertainty [K or °C].

$\overline{\sigma^2_{(S)}}$ : Mean Variance of the sample associated with  $U_{T(S)}$  [K<sup>2</sup>].

$\overline{\sigma_{(S)}}$ : Mean Standard Deviation of the sample associated with the Temperature Sensor Uncertainty ( $U_{T(S)}$ ) [K or °C].

$R_{SP}$ : Spatial Ratio or Ratio of Mean Variance of the sample due to the Temperature's Spatial Uncertainty ( $\overline{\sigma^2_{(SP)}}$ ) concerning the Mean Variance of the sample ( $\overline{\sigma_T^2}$ ).

$R_S$ : Sensor Ratio or Ratio of the Mean Variance of the sample due to Temperature Sensor Uncertainty ( $\overline{\sigma^2_{(S)}}$ ) concerning the Mean Variance of the sample ( $\overline{\sigma_T^2}$ ).

## Case study

### *Description of the monitoring system*

The monitored building is the west block of the University of the Basque Country (UPV/EHU) rectory (Figure 3). Eight EE071-HTPC (Table 1) sensors were installed within the existing building monitoring system to measure the Outdoor Air Temperature at several points. Seven of these installed sensors were protected against solar radiation using shields without mechanical ventilation and one with mechanical ventilation (ID sensor: 25). Table 2 shows the sensor references based on the ID sensor, height, cardinal orientation and building location. The sensors were installed around the building envelope at different heights and cardinal orientations (North (n), South (s) and West (w)). Figure 4 to 7 show the layout of the sensors.

The EE071-HTPC sensors with Modbus RS485 technology (The Modbus Organization, ) were integrated into the existing Building Automation System (BAS) implemented during the A2PBEER European project (a2pbeer.eu, ), with KNX protocol communication (KNX Association, ). A KNXRTU1K gateway was used for this (Table 1).

The experimental test for this study is described in detail in the Data in Brief article: 'Dataset of an in-use tertiary building collected from a detailed 3D Mobile



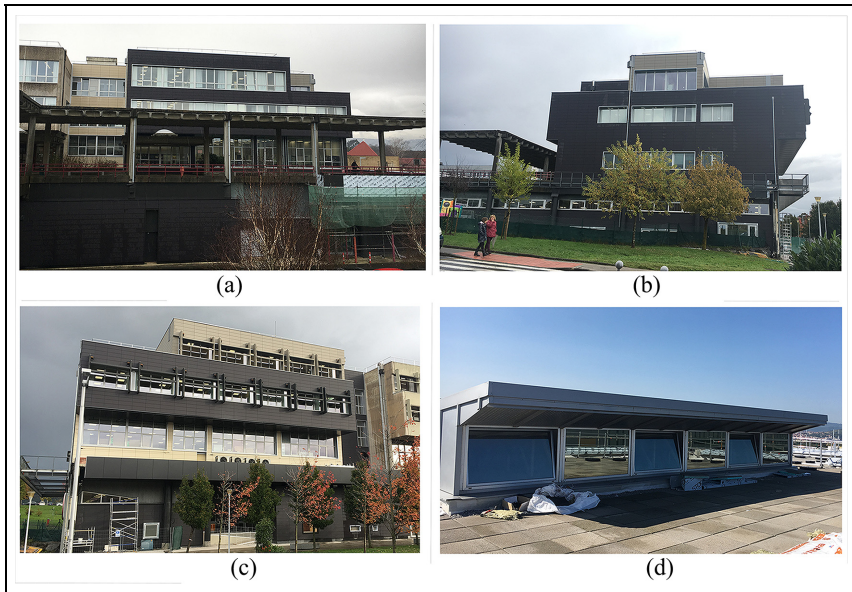


**Figure 3.** Upper view of the exterior sensor layout around the building envelope. Based on Giraldo-Soto et al. (2020) and Affordable and Adaptable Public Buildings through Energy Efficient Retrofitting (A2PBEER).

**Table 2.** Exterior (E) Layout of EE071-HTPC sensors installed around the building envelope.

Sensor reference	Façade (F)/ Roof (R) ***	Floor	Cardinal orientation	Sensor ID	Sensor manufacture reference
E.F1.n.20	F	1	n	20	EE071-HTP*
E.F1.n.21	F	1	n	21	EE071-HTP*
E.F1.w.22	F	1	w	22	EE071-HTP*
E.F1.s.23	F	1	s	23	EE071HTP*
E.F2.s.24	F	2	s	24	EE071-HTP*
E.R3.s.25	R	3	s	25	EE071-HTP**
E.R3.s.26	R	3	s	26	EE071-HTP*
E.R3.n.27	R	3	n	27	EE071-HTP*

Source: Based on Giraldo-Soto et al. (2020).

\*EE071-HTP are protected with solar radiation shielding without mechanical ventilation (RSHIELD – PM20 [28]).

\*\*EE071-HTP is protected by solar radiation shielding with mechanical ventilation (EE33-M Shielding (E + E Elektronik Ges.m.b.H., )).

\*\*\*All the sensors installed on the façade (F) are at a distance from the wall of at least 16 cm. These distances from the wall ensure we are not measuring the air temperature within the convective temperature boundary layer.

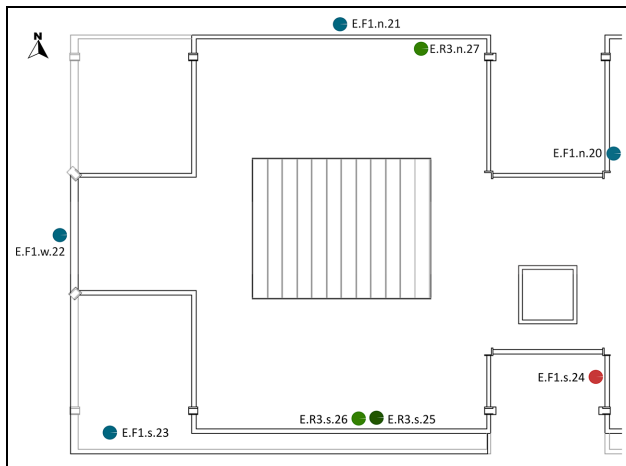


**Figure 4.** Upper view of the exterior sensor layout around the building envelope. Based on Giraldo-Soto et al. (2020) and Affordable and Adaptable Public Buildings through Energy Efficient Retrofitting (A2PBEER).

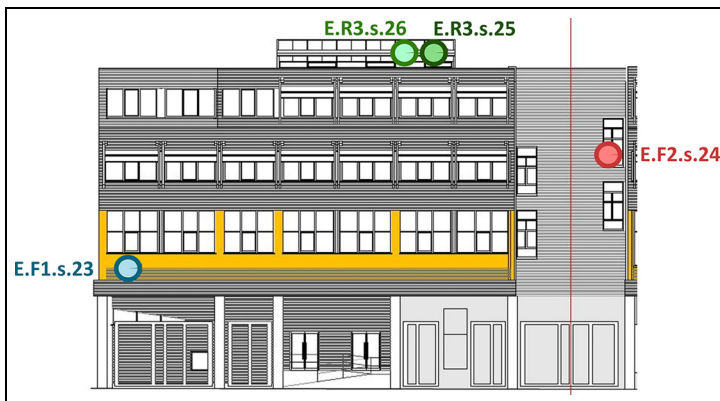


**Figure 5.** Exterior sensor layout on the south facade of the building. Based on Giraldo-Soto et al. (2020) and Affordable and Adaptable Public Buildings through Energy Efficient Retrofitting (A2PBEER).

Monitoring System and Building Automation System for indoor and outdoor air temperature analysis' (Giraldo-Soto et al., 2020). To carry out the studies on the  $T_{out}$  uncertainties of this work, the data sets generated by one of the experimental tests detailed in Giraldo-Soto et al. (2020) were used, the 'Exterior (E)Test'.

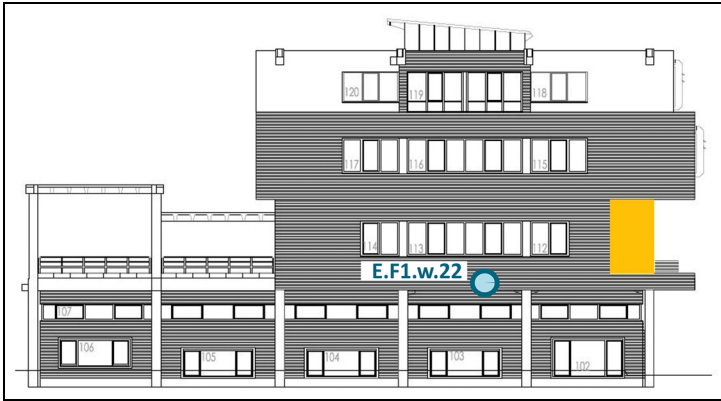


**Figure 6.** Exterior sensor layout on the west facade of the building. Based on Giraldo-Soto et al. (2020) and Affordable and Adaptable Public Buildings through Energy Efficient Retrofitting (A2PBEER).

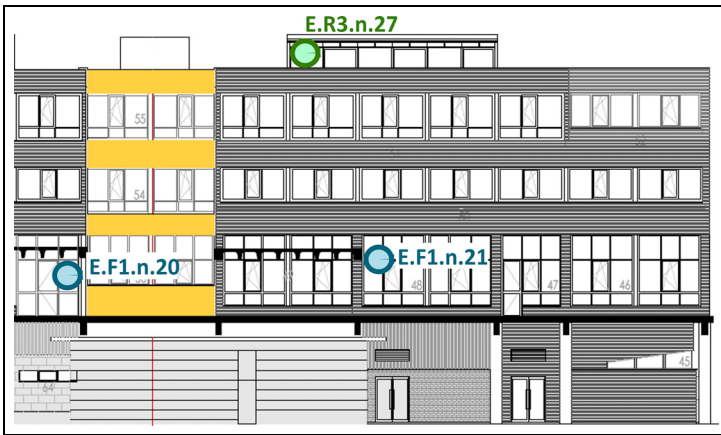


**Figure 7.** Exterior sensor layout on the north facade of the building. Based on Giraldo-Soto et al. (2020) and Affordable and Adaptable Public Buildings through Energy Efficient Retrofitting (A2PBEER).

## Results and discussions

The data analysis has been carried out on the data sets available in the data repository (Giraldo-Soto et al., 2020), specified and described in Giraldo-Soto et al. (2020). This section starts by validating the outdoor air temperature measurements performed by the sensors protected by solar radiation shields without mechanical ventilation (see Figure 8). It is followed by the estimation of the overall temperature uncertainty of the  $T_{out}$  for the BAV. A detailed analysis of the solar radiation



**Figure 8.** All the shielded sensors for the exterior monitoring system during the installation. The solar radiation shield with mechanical ventilation (on the left) on the mast can be seen together with a solar radiation shield without mechanical ventilation (on the right); these two sensors are already in their final position. Based on Giraldo-Soto et al. (2020).

effect on the  $T_{\text{out}}$  uncertainty value is included. Likewise, the Decoupling of the Temperature Uncertainty ( $U_T$ ) to estimate the Temperature's Spatial Uncertainty ( $U_{T(\text{SP})}$ ) from the Temperature Sensor Uncertainty ( $U_{T(S)}$ ) is presented at the end of this section.

In the analysed period, 407,664 data points were collected in 50,958 Instants of Time ( $t_j$ ) from 7th October 2019, at 12:42:20, to 6th January 2020, at 3:53:00, during the 'Exterior (E) Test' of (Giraldo-Soto et al., 2020). The results show three analysed cases for sub-periods with different  $t_j$  size: periods only With Solar Radiation (RAD ON) incidence, Without Solar Radiation (RAD OFF) incidence and also With and Without Solar Radiation (RAD ON-OFF) incidence, and whose sample sizes ( $N$ ) are equal to 17,527, 29,065 and 50,958 Instants of Time ( $t_j$ ), respectively.

In the RAD ON-OFF case, with a sample size equal to 50,958  $t_j$ , not all the  $t_j$  had solar radiation data registered from the sensor E.T9.m.1413 (Giraldo-Soto et al., 2020). Thus, 8% of these 50,958  $t_j$  do not have registered data for solar radiation; while the other 92% (46,952  $t_j$ ) do have registered solar radiation data.

The statistical analysis of the RAD ON-OFF case carried out in this section is based on a sample size equal to 50,958  $t_j$ . The RAD ON-OFF case, with a sample size equal to 46,952  $t_j$ , is also shown in order to analyse the  $U_T$  value of the  $T_{out}$  for the BAV with this smaller sample size, considering only the sample points where solar radiation measurements were available.

### Temperature Uncertainty ( $U_T$ ) analysis

*Temperature Uncertainty ( $U_T$ ) analysis for outdoor air temperature measurements protected with a solar radiation shield with and without mechanical ventilation.* Any radiation shield must be designed to provide an enclosure with an internal temperature that is uniform and equal to the outside air (Foken and Bange, 2021). The shielding should surround the thermometer and exclude radiant heat, precipitation and other phenomena that may influence the measurements. To ensure the shielding effect, they must be standardised to ISO 17714:2007 (2007). To demonstrate that the outdoor air temperature sensors protected against solar radiation only measure the air temperature by convection, thus excluding any effect of solar radiation, the analysed data were collected by the E.R3.s.25 and E.R3.s.26 sensors, with and without mechanical ventilation within the solar radiation shield, respectively. Data from October 7th, 2019, at 12:42:20, to January 6th, 2020, at 3:53:00 during the Exterior E test (Giraldo-Soto et al., 2020) was used. The methodology of the statistical analysis carried out is based on Subsection ‘Temperature Uncertainty ( $U_T$ ) analysis for outdoor air temperature measurements protected with a solar radiation shield with and without mechanical ventilation’. In Figure 9, it can be seen that:

- Figure 9(a) is the temperature evolution of both air temperature sensors and the horizontal global solar radiation measurements on October 08th, 2019, from 0:00 to 23:59 (UTC + 2). This top figure shows how the temperature signals of both sensors have the same behaviour and tendency.
- Figure 9(b) shows the histograms of the  $(\theta_{dvi})_{la}$  for the whole analysed period of the RAD ON-OFF case (E.R3.s.25 and E.R3.s.26 sensors). This middle figure shows how centred data  $((\theta_{dvi})_{la})$  tend to a normal distribution with a Mean ( $\mu_{t_j}$ ) equal to zero.
- Figure 9(c), here it is possible to appreciate how most  $(\theta_{dvi})_{la}$  are within the Manufacturer’s accuracy value ( $\pm 0.1^\circ\text{C}$ ).

The results of this statistical analysis are shown in Table 3 for different  $t_j$  samples, considering RAD ON-OFF, RAD ON and RAD OFF periods, respectively. The estimated  $U_T$  values are equal to  $\pm 0.091^\circ\text{C}$ ,  $\pm 0.112^\circ\text{C}$  and  $\pm 0.077^\circ\text{C}$  for RAD ON-OFF, RAD ON and RAD OFF periods, respectively. The case with the highest  $U_T$  value occurs in the periods with radiation incidence; while the lowest  $U_T$  value is for the periods without radiation incidence. Analysing the  $U_T$  Difference (UD) value regarding the solar radiation effect, it is possible to obtain two values

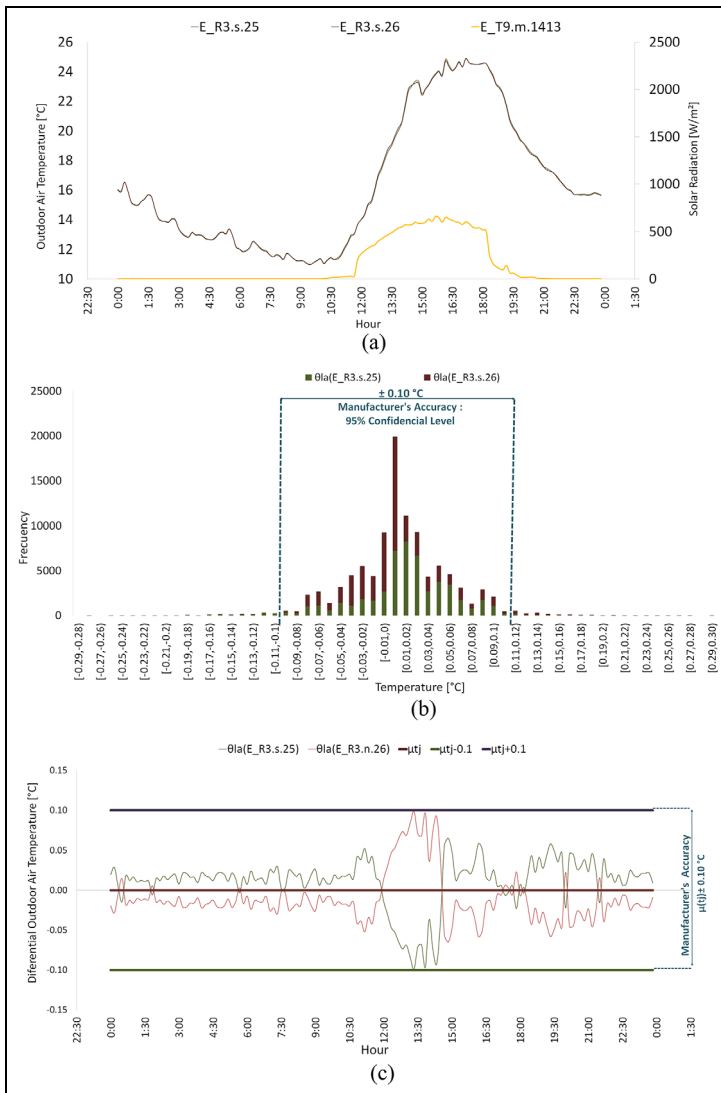


**Figure 9.** Panel (a) shows, on the left axis, the  $T_{dvi}$  evolution for October 08, 2019, from 0:00 to 23:59 (UTC + 2) of data collected from the E.R3.s.25 and E.R3.s.26 sensors; and on the right axis, the horizontal global solar radiation measurement. Panel (b) shows the histograms of  $T_{dvi}$  data, from E.R3.s.25 and E.R3.s.26 sensors, centred on  $(T_a)_{la}$ ,  $(\theta_{dvi})_{la}$ , for the RAD ON-OFF from October 7th, 2019, at 12:42:20 to January 6th, 2020, at 3:53:00 during the Exterior (E) test (Giraldo-Soto et al., 2020). Panel (c) represents the  $(\theta_{dvi})_{la}$  evolution of the E.R3.s.25 and E.R3.s.26 sensors on October 08, 2019, from 0:00 to 23:59 (UTC + 2) and the Mean ( $\mu_t$ ) with the Manufacturer's Accuracy (Manufacturer's Uncertainty) value ( $\pm 0.10^{\circ}\text{C}$ ).

**Table 3.** Temperature Uncertainty ( $U_T$ ) estimation for  $((\theta_{dv})_{la})$  with data centred on the Local Average Temperature  $((T_a)_{la})$  for the E.R3.s.25 and E.R3.s.26 sensors for each  $t_j$  in a BA, for the cases with and without solar radiation (RAD ON-OFF), with solar radiation (RAD ON) and without solar radiation (RAD OFF).

Data centred on the local average temperature for E.R3.s.25 and E.R3.s.26 (Roof (R))			
Statistical parameters	$t_j$ with RAD ON-OFF N = 50,958	$t_j$ with RAD ON N = 17,527	$t_j$ with RAD OFF N = 29,065
Z Measures by $t_j$	2	2	2
Mean $\bar{\mu}$ [°C] (equation (8))	0.000	0.000	0.000
Mean Variance $(\sigma^2_T)$ [K <sup>2</sup> ] (equation (9))	0.002	0.003	0.001
Mean Standard Deviation $(\sigma_T)$ [°C] (equation (10))	0.045	0.056	0.039
Temperature Uncertainty ( $U_T$ ) [°C] *(equation (11))	$\pm 0.091$	$\pm 0.112$	$\pm 0.077$
$((\theta_{dv})_{la})$ Min [°C]	-0.289	-0.230	-0.289
$((\theta_{dv})_{la})$ Max [°C]	0.290	0.230	0.290

\*Values of the Expanded Uncertainty, with  $k = 2$ .

to compare the RAD ON-OFF and RAD OFF periods with the RAD ON periods. The  $U_T$  Difference is obtained by subtracting the  $U_T$  value of periods with RAD ON-OFF and RAD OFF from the  $U_T$  of periods with radiation (RAD ON):

- The difference RAD ON and RAD OFF ( $UD_{rON-rOFF}$ ) is equal to 0.035°C.
- The difference RAD ON and RAD ON-OFF ( $UD_{rON-rON\_OFF}$ ) is equal to 0.022°C.

Both  $U_T$  Difference results are very low, considerably lower than the 0.10°C manufacturer's accuracy, which is a clear sign that the temperature measured by both sensors is the air temperature, excluding any solar radiation effect in any of the solar radiation shielding types, with and without mechanical ventilation. Likewise, this can be confirmed graphically in Figure 9(b), where 96.56% of the data are within the Manufacturer's Accuracy (Manufacturer's Uncertainty).

$T_{out}$  overall Temperature Uncertainty ( $U_T$ ) estimation for the whole Building Air Volume (BAV). This section calculates the overall uncertainty of the  $T_{out}$  measurement surrounding the tertiary building or the BAV. The statistical results of this section were obtained based on the methodology described in Subsection 'T<sub>out</sub> overall Temperature Uncertainty ( $U_T$ ) estimation for the whole Building Air Volume (BAV)' with data centred on  $(T_a)_{la}$  (equations (1) and (3)), which were calculated from the data of the eight temperature sensors installed randomly around the building envelope.

In Figure 10, it can be seen that:

- Figure 10(a) shows: the left axis  $T_{dvi}$  evolution during October 8th, 2019, from 0:00 to 23:59 (UTC + 2) of data collected from the E.F1.n.20, E.F1.n.21, E.F1.w.22, E.F1.s.23, E.F2.s.24, E.R3.s.25, E.R3.s.26 and E.R3.n.27 sensors; while the right axis shows the horizontal global solar radiation evolution.
- Figure 10(b) shows the histograms of the  $(\theta_{dvi})_{ia}$  of the eight installed temperature sensors, for the RAD ON-OFF case from October 7th, 2019, at 12:42:20 to January 6th, 2020, at 3:53:00 during the Exterior E test (Giraldo-Soto et al., 2020). This figure makes it possible to identify the fact that most of the data are outside the manufacturer's accuracy value ( $\pm 0.1^\circ\text{C}$ ).
- Figure 10(c) represents the  $(\theta_{dvi})_{ia}$  evolution of the E.F1.n.20, E.F1.n.21, E.F1.w.22, E.F1.s.23, E.F2.s.24, E.R3.s.25, E.R3.s.26 and E.R3.n.27 sensors on October 8th, 2019, from 0:00 to 23:59 (UTC + 2). Likewise, the Mean ( $\mu_{t_j}$ ) with the manufacturer's accuracy (Temperature Sensor Uncertainty ( $U_{T(S)}$ )) value ( $\pm 0.10^\circ\text{C}$ ) is also shown. Most of the  $(\theta_{dvi})_{ia}$  signals are outside the Mean  $\pm$  manufacturer's accuracy value ( $\mu_{t_j} \pm 0.10^\circ\text{C}$ ), since the uncertainties associated with the random errors are predominant.

Table 4 shows the results of the statistical analysis for the three studied cases, RAD ON-OFF ( $N = 50,958$ ), RAD ON ( $N = 17,527$ ) and RAD OFF ( $N = 29,065$ ). Likewise, this table shows the results for the RAD ON-OFF case for a sample size equal to  $46,952 t_j$ , where both temperature and global horizontal solar radiation measurements were collected within the sample size of  $50,958 t_j$ . Remember that some of the global horizontal solar radiation measurements were not registered. Additionally, Table 5 shows a relation of the average air temperature of the eight sensors,  $(\overline{T_a})_{ia}$ , with respect to the average air temperature of each sensor,  $\overline{T_a}$ .

In the case of the RAD ON and RAD OFF periods, the  $U_T$  values are equal to  $\pm 3.19^\circ\text{C}$  and  $\pm 1.38^\circ\text{C}$  (Table 4), respectively. The RAD ON period uncertainty value is considerably higher than for the RAD OFF period. The uncertainty of the  $T_{out}$  (remember that in this manuscript,  $T_{out}$  refers to the hypothetical homogeneous representative temperature surrounding the tertiary building) in periods with and without radiation (RAD ON-OFF) is equal to  $\pm 2.22^\circ\text{C}$  (Table 4). Thus, the minimum uncertainty for the  $T_{out}$  measurement is obtained during periods without solar radiation (this analysis considers RAD-OFF to be when the locally measured global horizontal radiation is below  $50 \text{ W/m}^2$ ). This result shows how solar radiation increases the  $U_T$  value of  $T_{out}$ .

Furthermore, comparing the  $U_T$  value equal to  $\pm 2.22^\circ\text{C}$  of the sample with  $50,958$  concerning the  $U_T$  value of  $\pm 2.24^\circ\text{C}$  (Table 4) of the sample size of  $46,592$ , it is possible to affirm that the  $U_T$  equal to  $\pm 2.22^\circ\text{C}$  is a consistent value of the  $T_{out}$  uncertainty for the RAD ON-OFF case.

From (Table 4), it can be stated with 95% confidence that the average temperature of the outdoor air surrounding the studied building during the monitoring



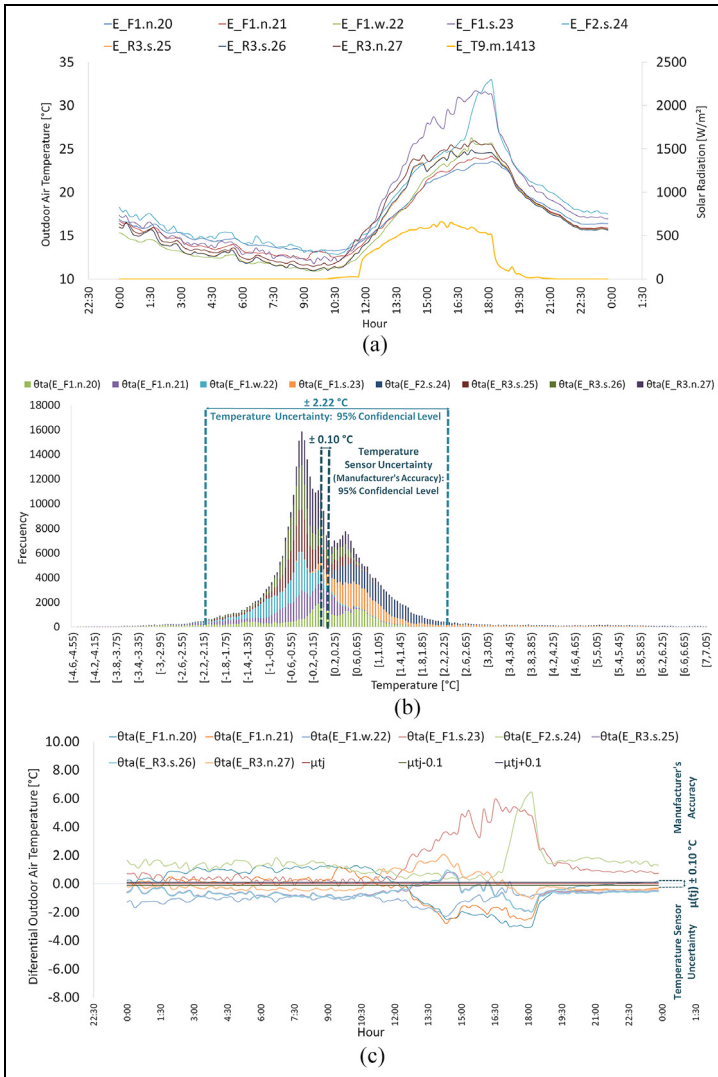


**Figure 10.** Panel (a) shows the left axis is the  $T_{dvi}$  evolution during October 8th, 2019, from 0:00 to 23:59 (UTC + 2) of data collected from the E.F1.n.20, E.F1.n.21, E.F1.w.22, E.F1.s.23, E.F2.s.24, E.R3.s.25, E.R3.s.26 and E.R3.n.27 sensors; while the right axis shows the horizontal global solar radiation evolution. Panel (b) shows the histogram of the  $T_{dvi}$  data, of the E.F1.n.20, E.F1.n.21, E.F1.w.22, E.F1.s.23, E.F2.s.24, E.R3.s.25, E.R3.s.26 and E.R3.n.27 sensors, centred on  $(T_a)_{ta}$ ,  $(\theta_{dvi})_{ta}$ , for the RAD ON-OFF case from October 7th, 2019, at 12:42:20 to January 6th, 2020, 3:53:00 during the Exterior E test (Giraldo-Soto et al., 2020). Panel (c) represents the  $(\theta_{dvi})_{ta}$  evolution of the E.F1.n.20, E.F1.n.21, E.F1.w.22, E.F1.s.23, E.F2.s.24, E.R3.s.25, E.R3.s.26 and E.R3.n.27 sensors on October 8th, 2019, from 0:00 to 23:59 (UTC + 2) and the Mean ( $\mu_{tj}$ ) with the manufacturer's accuracy value ( $\pm 0.1^\circ\text{C}$ ).

**Table 4.** Overall Temperature Uncertainty ( $U_T$ ) results for the whole Building Air Volume (BAV) with data centred on the Total Average Temperature ( $(T_{a,ta})$ ) for each  $t_j$ , with and without solar radiation.

Overall Temperature Uncertainty ( $U_T$ ) results for the whole Building Air Volume (BAV)									
Case	Z by $t_j$	$(T_{a,ta})$ [°C]* (equation (1))	$\bar{\mu}$ [°C] (equation (8))	$\bar{\sigma}^2_T$ [K <sup>2</sup> ] (equation (9))	$\bar{\sigma}_T$ [°C] (equation (10))	$U_T$ [°C]** (equation (11))	Min	Max	
$t_j$ with RAD ON-OFF N = 50,958	8	17.810	0.000	1.230	1.109	± 2.22	-4.501	7.079	
$t_j$ with RAD ON-OFF N = 46,592	8	18.09	0.000	1.254	1.120	± 2.24	-4.501	7.079	
$t_j$ with RAD ON N = 17,527	8	20.44	0.000	2.541	1.594	± 3.19	-4.501	7.079	
$t_j$ with RAD OFF N = 29,065	8	16.67	0.000	0.478	0.691	± 1.38	-2.899	5.396	

\*Average of all the Average Temperatures ( $(T_{a,ta})$  (equation (1)) considered in each of the analysis.

\*\*Values of the Expanded Uncertainty with  $k = 2$ .

**Table 5.** Average Temperatures ( $(T_{a,ta})$ ) and the Average temperature ( $(T_a)$ ) of outdoor air temperature sensors for each studied case.

Case	$(T_{a,ta})$ [°C]* (equation (1))	$(T_{a,E,F1,n,20})$ [°C]	$(T_{a,E,F1,n,21})$ [°C]	$(T_{a,E,F1,w,22})$ [°C]	$(T_{a,E,F1,s,23})$ [°C]	$(T_{a,E,F2,s,24})$ [°C]	$(T_{a,E,R3,s,25})$ [°C]	$(T_{a,E,R3,s,26})$ [°C]	$(T_{a,E,R3,n,27})$ [°C]
$t_j$ with RAD ON-OFF N = 50,958	17.81	17.61	17.22	17.14	18.95	19.09	17.40	17.39	17.68
$t_j$ with RAD ON N = 17,527	20.44	19.36	19.22	19.92	22.52	22.19	19.91	19.96	20.42
$t_j$ with RAD OFF N = 29,065	16.67	16.93	16.42	15.90	17.26	17.68	16.36	16.32	16.51

\*Average of all the Average Temperatures ( $(T_{a,ta})$  (equation (1)) considered in each of the analysis.

**Table 6.** Statistical results from manufacturer's accuracy of the EE071-HTPC sensor.

Manufacturer's Accuracy Statistical Analysis with a confidence level of 95% using $k = 2$	Sensor reference EE071-HTPC*	Units
Expanded Uncertainty ( $U_{T(S)}$ ) (manufacturer data)	$\pm 0.10$	[°C]
Mean Standard Deviation ( $\overline{\sigma_{(S)}}$ ) (equation (11))	<b>0.0500</b>	[°C]
Mean Variance ( $\overline{\sigma^2_{(S)}}$ ) (Equation. (10))	<b>0.0025</b>	[K <sup>2</sup> ]

\*Estimated and obtained values based on the sensor data sheet, where the Expanded Uncertainty was estimated with  $k = 2$ .

period, comprised from October 7th, 2019, at 12:42:20 to January 6th, 2020, 3:53:00, was  $17.81 \pm 2.22^\circ\text{C}$ . Note that the uncertainty band of this  $T_{\text{out}}$  is much higher than the  $\pm 0.1^\circ\text{C}$  uncertainty value given by the sensors' manufacturer, which is generally used as the overall measurement uncertainty.

Finally, from (Table 5), it can be stated that, for this particular building, the best position to place the outdoor temperature sensor would be the north area of the roof (sensor E.R3.n.27). This is the position where the individual temperature measurement is closest to the mean of the eight sensors surrounding the building. Obviously, this is a case specific result.

### Temperature Sensors Uncertainty ( $U_{T(S)}$ ) analysis

The Temperature Sensor Uncertainty ( $U_{T(S)}$ ) value considers the uncertainty due to systematic errors. This value is given by the sensor manufacturer through the sensor accuracy and can also be obtained experimentally (Giraldo-Soto, 2021). The results shown in this section were obtained based on the methodology set out in Subsection 'Temperature Sensor Uncertainty ( $U_{T(S)}$ ) analysis'. This section starts with the statistical parameters of  $U_{T(S)}$  given by the manufacturer, which is equal to  $\pm 0.10^\circ\text{C}$ .

Table 6 shows the Mean Variance equals  $0.0025\text{K}^2$  and the Mean Standard Deviation equals  $0.05^\circ\text{C}$ , calculated from the Manufacturer's Accuracy data. This  $U_{T(S)}$  value is estimated with a confidence level equal to 95%, so the  $k$  value equals 2 (Modbus RTU humidity and Temperature Probe). The methodology applied to make this estimation is based on equations (9) to (11).

### Decoupling the Temperature Uncertainty ( $U_T$ ) by means of the Temperature Sensor Uncertainty ( $U_{T(S)}$ ) to estimate the Temperature's Spatial Uncertainty ( $U_{T(SP)}$ ) of the whole Building Air Volume (BAV)

In this section, the decoupling method was carried out to estimate the Temperature's Spatial Uncertainty ( $U_{T(SP)}$ ) in order to know the influence of the random errors on the overall Temperature Uncertainty ( $U_T$ ), together with the systematic errors through the Temperature Sensor Uncertainty ( $U_{T(S)}$ ).

The results of decoupling the Temperature Uncertainty ( $U_T$ ) using the Temperature Sensor Uncertainty ( $U_{T(S)}$ ) to estimate the Temperature's Spatial Uncertainty ( $U_{T(SP)}$ ) are shown in Table 7. To obtain the results of the decoupling method for the RAD ON-OFF, RAD ON and RAD OFF cases, the  $T_{out}$  overall Temperature Uncertainty ( $U_T$ ) values, and their associated Mean Variance and Mean Standard Deviation values (Table 4), have been taken into account. Decoupling the  $U_T$  value has allowed us to obtain the uncertainty due to the random errors that affect the  $T_{out}$  measurement, called in this document, Temperature's Spatial Uncertainty ( $U_{T(SP)}$ ). This value has been calculated using the  $\sigma^2_{(S)}$  value equal to  $\pm 0.0025 \text{ K}^2$  (from Table 6).

The  $U_{T(SP)}$  (equation (13)),  $R_S$  (equation (16)) and  $R_{SP}$  (equation (17)) values were estimated based on the methodology of Section 'Decoupling the overall Temperature Uncertainty ( $U_T$ ) by means of the Temperature Sensor Uncertainty ( $U_{T(S)}$ ) to estimate the Temperature's Spatial Uncertainty ( $U_{T(SP)}$ ) for the whole Building Air Volume (BAV)', and the results are shown in Table 7. For the RAD ON-OFF case, the  $U_{T(SP)}$  value is equal to  $\pm 2.22^\circ\text{C}$ , while the  $R_S$  and  $R_{SP}$  values are equal to 0.20% and 99.80%, respectively. The  $U_{T(SP)}$  value for the RAD ON case is equal to  $\pm 3.19^\circ\text{C}$ , the  $R_S$  and  $R_{SP}$  values are equal to 0.10% and 99.90%, respectively. For the RAD OFF case, the  $U_{T(SP)}$  value is equal to  $\pm 1.38^\circ\text{C}$ , while the  $R_S$  and  $R_{SP}$  values are equal to 0.52% and 99.48%, respectively. The  $R_{SP}$  values for the three studied cases are three orders of magnitude higher than the  $R_S$  values; thus, the  $T_{out}$  measurement uncertainties associated with the random errors are those with the main incidence of the  $T_{out}$  measurement. The systematic errors can be considered negligible in this case.

Additionally, taking into account that the estimated  $U_{T(SP)}$  values of the air temperature for the different closed indoor volumes of this studied tertiary building are between  $\pm 0.67^\circ\text{C}$  and  $\pm 1.05^\circ\text{C}$  (Giraldo-Soto et al., 2022), the  $U_{T(SP)}$  values of air surrounding the building are considerably greater (Table 7).

**Table 7.** Decoupling of  $T_{out}$  measurement uncertainty with data centred on the Total Average Temperature ( $(T_a)_{tot}$ ) for the eight installed sensors in each  $t_j$  with and without solar radiation.

Decoupling of $T_{out}$ measurement to estimate the Temperature's Spatial Uncertainty									
Case	Temperature Sensor Uncertainty ( $U_{T(S)}$ ) from Manufacturer's Accuracy (Table 6): $\overline{\sigma^2_{T(S)}} = 0.0025 K^2 \cdot \overline{\sigma_{T(S)}} = 0.05^\circ C$ ; $U_{T(S)} = \pm 0.1^\circ C$								
	$\overline{\sigma^2_T} [K^2]$ (Table 4)	$\overline{\sigma_T} [^\circ C]$ (Table 4)	$U_T [^\circ C]$ (Table 4)	$\overline{\sigma^2_{(SP)}} [K^2]$ (equation (13))	$\overline{\sigma_{SP}} [^\circ C]$ (equation (10))	$U_{T(SP)} [^\circ C]$ (equation (11))	$R_S^{**}$ (equation (16))	$R_{SP}^{***}$ (equation (17))	
$t_j$ with RAD ON-OFF N = 50,958	1.23028	1.10918	$\pm 2.22$	1.22778	1.10805	$\pm 2.22$	<b>0.20%</b>	<b>99.80%</b>	
$t_j$ with RAD ON N = 17,527	2.54138	1.59417	$\pm 3.19$	2.53888	1.59339	$\pm 3.19$	<b>0.10%</b>	<b>99.90%</b>	
$t_j$ with RAD OFF N = 29,065	0.47779	0.69122	$\pm 1.38$	0.47529	0.68941	$\pm 1.38$	<b>0.52%</b>	<b>99.48%</b>	

To appreciate the differences between the different values, some of the results are shown with five decimals.

\*Values of the Expanded Uncertainty with  $k = 2$ .

\*\*The value of the each ratio is expressed as a percentage.

## Conclusions

In the literature review of this manuscript, it is highlighted that the practice of considering the outdoor air temperature surrounding the building envelope as homogeneous is well established. In addition, when measured, it is common practice to have a unique measurement representing this hypothetical homogeneous outdoor air temperature surrounding the building envelope (namely  $T_{\text{out}}$ ). Furthermore, the uncertainty associated with this measurement (when provided within the research) is usually limited to the accuracy of the sensor given by the manufacturer. In this manuscript, an overall uncertainty of this hypothetical homogeneous outdoor air temperature ( $T_{\text{out}}$ ) measurement has been defined and quantified. For this, the existing spatial variability of the outdoor air temperature measurements around a building envelope has been defined as a random error. Likewise,  $T_{\text{out}}$  has been defined as the average temperature of several sensors located randomly around the building envelope. Then, the total variability of these measurements regarding  $T_{\text{out}}$  at a given time instant has been linked through the GUM method to the overall Temperature Uncertainty ( $U_T$ ) of the  $T_{\text{out}}$  measurement. The uncertainty associated with the systematic errors of the  $T_{\text{out}}$  measurement has been defined as the Temperature Sensor Uncertainty ( $U_{T(S)}$ ) and this is associated with the sensor accuracy. Based on these hypotheses, a detailed statistical procedure has been developed to estimate these two uncertainties. Finally, an uncertainty decoupling method has also been developed, which allows the uncertainty associated with random errors (Temperature's Spatial Uncertainty ( $U_{T(SP)}$ )) based on ( $U_T$ ) and ( $U_{T(S)}$ ) values to be estimated.

The method has been applied to the  $T_{\text{out}}$  measurement of a four-floor building, where eight high-precision temperature sensors (with a  $\pm 0.1^\circ\text{C}$  accuracy;  $U_{T(S)} = 0.1^\circ\text{C}$ ) were randomly installed around its envelope. The sensors were simultaneously monitoring the outdoor air temperature for several weeks. The results show that the overall Temperature Uncertainty of  $T_{\text{out}}$  is equal to  $\pm 2.22^\circ\text{C}$  (in which the systematic and random errors are included) for the whole monitored period. Thus, the main conclusion reported is that only considering the sensor manufacturer's accuracy as the overall uncertainty of the  $T_{\text{out}}$  measurement leads to strongly underestimating the  $T_{\text{out}}$  measurements' uncertainty value.

Additionally, the monitoring period was divided into two sub-periods: one considers all the measurement instants with solar radiation incidence, and the other considers all the measurement instants without solar radiation incidence. Analysing the sub-period with solar radiation, this overall Temperature Uncertainty increases to  $\pm 3.19^\circ\text{C}$ ; while for the sub-period without solar radiation incidence, it decreases to  $\pm 1.38^\circ\text{C}$ . Thus, solar radiation incidence is one of the main random uncertainty sources (or physical effects that generate spatial variability around the outdoor air temperature surrounding a building envelope) in the  $T_{\text{out}}$  measurement. Consequently, research studies that only consider cloudy periods and night time will have a lower measurement uncertainty of outdoor air temperature, thus improving the reliability of their estimates. Furthermore, this also

reflects the importance of estimating the HTC on cloudy days to reduce the uncertainty of its estimation, which will allow great progress towards the development of more reliable methods for estimating the HTC and its uncertainty.

Finally, thanks to the developed Temperature Uncertainty decoupling method, it has been possible to estimate the Temperature Spatial Uncertainties (which include only the random errors) of  $T_{\text{out}}$ ; these being equal to  $\pm 2.22^{\circ}\text{C}$  in periods with and without solar radiation incidence,  $\pm 3.19^{\circ}\text{C}$  in periods with solar radiation incidence and  $\pm 1.38^{\circ}\text{C}$  in periods without solar radiation incidence. Likewise, the weight of the Temperature Spatial Uncertainties represents 99.93%, 99.97% and 99.82% of the overall Temperature Uncertainty in periods with and without solar radiation incidence, with solar radiation incidence and without solar radiation incidence, respectively. This analysis of the weight the random errors have in the overall Temperature Uncertainty of  $T_{\text{out}}$  can quantify to what extent we are underestimating the  $T_{\text{out}}$  overall uncertainty when only considering the sensor manufacturer's accuracy as the overall uncertainty of the  $T_{\text{out}}$  measurements.

### Auhtor contributions

**Catalina Giraldo-Soto:** Conceptualization, methodology, software, validation, formal analysis, investigation, resources, data curation, writing – original draft, visualization, funding acquisition. **Aitor Ekoreka:** Conceptualization, validation, resources, writing – review & editing, supervision, project administration, funding acquisition. **Laurent Mora:** Conceptualization, methodology, validation, writing – review & editing, supervision, project administration. **Amaia Uriarte:** Resources, writing – review & editing, funding acquisition. **Pablo Eguia-Oller:** Writing – review & editing, funding acquisition. **Christopher Gorse:** Writing – review & editing, funding acquisition.


### Declaration of conflicting interests


The author(s) declared no potential conflicts of interest with respect to the research, authorship, and/or publication of this article.

### Funding

The author(s) disclosed receipt of the following financial support for the research, authorship, and/or publication of this article: This publication is part of the R + D + i project PID2021-126739OB-C22, financed by MICIU//AEI/10.13039/501100011033/ and 'ERDF A way of making Europe'. The corresponding author also acknowledges the support provided by the University of the Basque Country and the University of Bordeaux through a scholarship granted to Dr. Catalina Giraldo-Soto to complete her PhD degree through the Framework Agreement: Euro-regional Campus of Excellence within the context of their respective excellence projects, Euskampus and IdEx Bordeaux. Funder reference: PIFBUR 16/26. University of the Basque Country (UPV/EHU). Likewise, it acknowledges the support the Basque Government provides through a post-doctoral fellowship granted to Dr. Catalina Giraldo-Soto, which funding is awarded according to the order dated July 6, 2021, from the Minister of Education. Funder reference: POS\_2021\_1\_0019, POS\_2022\_2\_0043 and POS\_2023\_2\_0025

## ORCID iDs

Catalina Giraldo-Soto  <https://orcid.org/0000-0003-3275-1856>

Aitor Erkoreka  <https://orcid.org/0000-0001-5158-0170>

## References

- a2pbeer.eu. Affordable and Adaptable Public Buildings through Energy Efficient Retrofitting (A2PBEER). Available at: <https://cordis.europa.eu/project/id/609060/news/es> (accessed 6 August 2024). (accessed 10 May 2024).
- ASHRAE. 2021 *ASHRAE Handbook: Fundamentals*.
- Bakkush AFE, Bondinuba FK and Harris DJ (2015) The effect of outdoor air temperature on the thermal performance of a residential building. *Journal of Multidisciplinary Engineering Science and Technology* 2(9): 3159–3240.
- Bauwens G and Roels S (2014) Co-heating test: A state-of-the-art. *Energy and Buildings* 82: 163–172.
- BIPM. Guide to the expression of uncertainty in measurement (GUM). Available at: <https://www.bipm.org/en/publications/guides/gum.html> (accessed 6 August 2024).
- Borkowski M and Piłat AK (2022) Customized data center cooling system operating at significant outdoor temperature fluctuations. *Applied Energy* 306: 117975.
- Calama-González CM, León-Rodríguez ÁL and Suárez R (2021) Indoor environmental assessment: Comparing ventilation scenarios in pre- and post-retrofitted dwellings through test cells. *Journal of Building Engineering* 43: 103148.
- Chapman AJ (1984) *Heat Transfer*. Macmillan.
- Chung D, Wen J and Lo LCJ (2023) Examining the impact of stochastic multi-year weather and air infiltration on hygrothermal moisture risks. *Journal of Building Physics* 47(1): 4–35.
- DEEI. Pasarelas. Available at: [https://deei.es/?product\\_cat=pasarelas](https://deei.es/?product_cat=pasarelas) (accessed 6 August 2024).
- E + E Elektronik Ges.m.b.H. Available at: <https://www.epluse.com/news/press/press-releases/info/humidity-and-temperature-transmitter-for-demanding-meteorological-applications-55/> (accessed 6 August 2024).
- E + E Elektronik Ges.m.b.H. EE33-M: Humidity and temperature transmitter for high-end meteorological applications. Available at: <https://www.epluse.com/news/press/press-releases/info/humidity-and-temperature-transmitter-for-demanding-meteorological-applications-55/> (accessed 6 August 2024).
- E + E Elektronik Ges.m.b.H. Humidity and temperature probe with digital interface. Available at: <https://www.epluse.com/en/products/humidity-instruments/humidity-measuring-modules/ee072/> (accessed 6 August 2024).
- Foken T and Bange J (2021) Temperature sensors. In: T Foken (ed.) *Springer Handbook of Atmospheric Measurements*. Springer Handbooks. Cham: Springer International Publishing, pp. 183–208.
- Ghosh A, Norton B and Duffy A (2015) Measured overall heat transfer coefficient of a suspended particle device switchable glazing. *Applied Energy* 159: 362–369.
- Giraldo-Soto C (2021) *Optimized monitoring techniques and data analysis development for in-situ characterization of the building envelope's real energetic behaviour*. Doctoral thesis, University of Bordeaux and University of Basque Country. Available at: <http://www.theses.fr/2021BORD0041> (accessed 26 January 2024).



- Giraldo-Soto C, Erkoreka A, Barragan A, et al. (2020) Data repository. Dataset of an in-use tertiary building collected from a detailed 3D Mobile Monitoring System and Building Automation System for indoor and outdoor air temperature analysis. *Data in Brief* 31: 105907.
- Giraldo-Soto C, Erkoreka A, Mora L, et al. (2018) monitoring system analysis for evaluating a building's envelope energy performance through estimation of its heat loss coefficient. *Sensors* 18(7): 2360.
- Giraldo-Soto C, Mora L, Erkoreka A, et al. (2022) Overall uncertainty analysis of zonal indoor air temperature measurement in an in-use office building. *Building and Environment* 219: 109123.
- He X, Li A and Ning Y (2020) Optimization of outdoor design temperature for summer ventilation for undersea road tunnel using field measurement and statistics. *Building and Environment* 167: 106457.
- Housez PP, Pont U and Mahdavi A (2014) A comparison of projected and actual energy performance of buildings after thermal retrofit measures. *Journal of Building Physics* 38(2): 138–155.
- Huang Z, Gou Z and Cheng B (2020) An investigation of outdoor thermal environments with different ground surfaces in the hot summer-cold winter climate region. *Journal of Building Engineering* 27: 100994.
- ISO 17714:2007 (2007) Meteorology – Air temperature measurements – Test methods for comparing the performance of thermometer shields/screens and defining important characteristics. Available at: <https://www.iso.org/cms/render/live/en/sites/isoorg/contents/data/standard/03/14/31498.html> (accessed 7 January 2024).
- ISO Standard 9869-1 (2014) Thermal insulation – Building elements – In-situ measurement of thermal resistance and thermal transmittance – Part 1: Heat flow meter method.
- Jack R, Loveday D, Allinson D, et al. (2018) First evidence for the reliability of building co-heating tests. *Building Research & Information* 46(4): 383–401.
- Juricic S, Goffart J, Rouchier S, et al. (2021) Influence of natural weather variability on the thermal characterisation of a building envelope. *Applied Energy* 288: 116582.
- KNX Association. Available at: <https://www.knx.org/> (accessed 6 August 2024).
- Lai P-Y, Koh JH, Koh WS, et al. (2020) Effectively modeling surface temperature and evaluating mean radiant temperature in tropical outdoor industrial environments. *Building and Environment* 169: 106277.
- Li Z, Wei W, Wang W, et al. (2023) A method for sizing air source heat pump considering the joint effect of outdoor air temperature and relative humidity. *Journal of Building Engineering* 65: 105815.
- Modbus RTU Humidity and Temperature Probe. Available at: [https://www.epluse.com/fileadmin/data/product/ee071/BA\\_EE071\\_e.pdf](https://www.epluse.com/fileadmin/data/product/ee071/BA_EE071_e.pdf) (accessed 22 February 2024).
- Pandas. Pandas documentation. Available at: <https://pandas.pydata.org/pandas-docs/stable/index.html#> (accessed 6 August 2024).
- Python.org. Python.org. Available at: <https://www.python.org/> (accessed 6 August 2024).
- Sansaniwal SK, Mathur J and Mathur S (2021) Quantifying occupant's adaptive actions for controlling indoor environment in naturally ventilated buildings under composite climate of India. *Journal of Building Engineering* 41: 102399.
- Scipy. Statistical functions (scipy.stats). Reference guide. Available at: <https://docs.scipy.org/doc/scipy/reference/stats.html?highlight=stats#module-scipy.stats> (accessed 6 August 2024).

- Sougkakis V, Meulemans J, Wood C, et al. (2021) Field testing of the QUB method for assessing the thermal performance of dwellings: In situ measurements of the heat transfer coefficient of a circa 1950s detached house in UK. *Energy and Buildings* 230: 110540.
- The Modbus Organization. Available at: <http://www.modbus.org/> (accessed 6 August 2024).
- Vivek T and Balaji K (2023) Influence of cooling surface area on indoor air and surface heat transfer characteristics of a thermally activated building system in warm and humid zones: An Experimental study. *Journal of Building Physics* 47(2): 204–229.
- Yan H, Yang L, Zheng W, et al. (2016) Influence of outdoor temperature on the indoor environment and thermal adaptation in Chinese residential buildings during the heating season. *Energy and Buildings* 116: 133–140.
- Yang S, Wan MP, Ng BF, et al. (2020) Experimental study of model predictive control for an air-conditioning system with dedicated outdoor air system. *Applied Energy* 257: 113920.
- Zhang J, Cui P and Song H (2020) Impact of urban morphology on outdoor air temperature and microclimate optimization strategy base on Pareto optimality in Northeast China. *Building and Environment* 180: 107035.

## Appendix

### Acronyms

Acronym	Meaning
ASHRAE	American Society of Heating, Refrigerating and Air-Conditioning Engineers
BA	Building areas
BAV	Building air volume or air surrounding the building
$dv_i$	Volume differential
E	Exterior
ET	Exterior together
ISO	International Organization for Standardization
GUM	Guide to the expression of uncertainty in measurement
HTC	Heat transfer coefficient
$k$	Coverage factor
MMS	Mobile monitoring system
$\mu$	Mean
$\bar{\mu}$	Global mean or mean of the sample
$\mu_{t_j}$	Mean of temperature differentials for each instants of time
$n$	North
$N$	Number of instants of time or sample size
$p$	Number of $Tdv_i$ measurements around the BAV for each $t_j$
ppm	Parts per million
$q$	Number of $Tdv_i$ measurements in a BA for each $t_j$
RAD OFF	Without solar radiation
RAD ON	With solar radiation
RAD ON-OFF	With and without solar radiation
RH	Relative humidity

(continued)

## Appendix. (continued)

Acronym	Meaning
$R_S$	Sensor ratio or ratio of mean variance associated with temperature sensor uncertainty with respect to mean variance associated with temperature uncertainty
$R_{Sp}$	Spatial ratio or ratio of mean variance associated with temperature's spatial uncertainty with respect to mean variance associated with temperature uncertainty
s	South
$\sigma$	Standard deviation
$\sigma^2$	Variance
$\bar{\sigma}$	Mean standard deviation of the sample
$\overline{\sigma^2}$	Mean variance of the sample
$\overline{\sigma_T}$	Mean standard deviation of sample associated with temperature uncertainty [K or °C]
$\overline{\sigma^2_T}$	Mean Variance of sample associated with temperature uncertainty [K <sup>2</sup> ]
$\overline{\sigma_{(S)}}$	Mean Standard deviation of the sample associated with temperature sensor uncertainty
$\overline{\sigma^2_{(S)}}$	Mean variance of the sample associated with temperature sensor uncertainty
$\overline{\sigma_{(SP)}}$	Mean standard deviation of the sample associated with temperature's spatial uncertainty
$\overline{\sigma^2_{(SP)}}$	Mean variance of the sample associated with temperature's spatial uncertainty
$\sigma_{t_j}$	Standard deviation of temperature differentials for each instant of time ( $t_j$ )
$\sigma^2_{t_j}$	Variance of temperature differentials for each instant of time ( $t_j$ )
$\sigma^2_{t_j(S)}$	Variance of temperature differentials for each instant of time ( $t_j$ ) associated with temperature sensor uncertainty
$\sigma^2_{t_j(SP)}$	Variance of temperature differentials for each instant of time ( $t_j$ ) associated with temperature's spatial uncertainty
$T_{out}$	Hypothetical homogenous outdoor air temperature surrounding a building envelope in a certain instant of time defined as the average temperature of several sensors located randomly around the building envelope [K or °C]
$T_a$	Average temperature [K or °C]
$(T_a)_{la}$	Local average temperature of $T_{dv_i}$ measurements collected on a BA for each $t_j$ [K or °C]
$(T_a)_{ta}$	Total average temperature of $T_{dv_i}$ measurements collected around the BAV for each $t_j$ [K or °C]
$T_{dv_i}$	Sensor Temperature Measurements of a Differential Volume ( $dv_i$ ) [K or °C]
$t_j$	Instants of Time
$\theta_{dv_i}$	Temperature differential [K or °C]
$(\theta_{dv_i})_{la}$	Temperature differential of a $T_{dv_i}$ measurement centred on local average temperature ( $(T_a)_{la}$ ) of a BA for each $t_j$ [K or °C]
$(\theta_{dv_i})_{ta}$	Temperature differential of a $T_{dv_i}$ measurement centred on total average temperature ( $(T_a)_{ta}$ ) of a BAV for each $t_j$ [K or °C]
U	Standard uncertainty
UPV/EHU	University of the Basque Country
$\bar{U}$	Expanded uncertainty

(continued)

**Appendix.** (continued)

Acronym	Meaning
$U_T$	Temperature uncertainty
$U_{T(SP)}$	Temperature's spatial uncertainty
$U_{T(S)}$	Temperature sensor uncertainty
$w$	West
$Z$	Number of temperature measurements ( $T_{dv_i}$ or $\theta_{dv_i}$ ) in each $t_j$ [for $(T_a)_{ta}$ ( $Z = p$ ) and for $(T_a)_{la}$ ( $Z = q$ )]